Microscopic study of the superconducting state of the iron pnictide RbFe₂As₂ via muon spin rotation

Z. Shermadini, ^{1,2} J. Kanter, ³ C. Baines, ¹ M. Bendele, ^{1,4} Z. Bukowski, ³ R. Khasanov, ¹ H.-H. Klauss, ² H. Luetkens, ¹ H. Maeter, ² G. Pascua, ¹ B. Batlogg, ³ and A. Amato ¹

¹Laboratory for Muon Spin Spectroscopy, Paul Scherrer Institute, CH-5232 Villigen PSI, Switzerland

²Institut für Festkörperphysik, TU Dresden, D-01069 Dresden, Germany

³Laboratory for Solid State Physics, ETH Zürich, CH-8093 Zürich, Switzerland

⁴Physik-Institut, Universität Zürich, Winterthurerstrasse 190, CH-8057 Zürich, Switzerland

(Received 21 May 2010; revised manuscript received 16 August 2010; published 28 October 2010)

A study of the temperature and field dependence of the penetration depth λ of the superconductor RbFe₂As₂(T_c =2.52 K) was carried out by means of muon-spin rotation measurements. In addition to the zero-temperature value of the penetration depth $\lambda(0)$ =267(5) nm, a determination of the upper critical field $B_{c2}(0)$ =2.6(2) T was obtained. The temperature dependence of the superconducting carrier concentration is discussed within the framework of a multigap scenario. Compared to the other "122" systems which exhibit much higher Fermi level, a strong reduction in the large gap BCS ratio $2\Delta/k_BT_c$ is observed. This is interpreted as a consequence of the absence of interband processes. Indications of possible pair-breaking effect are also discussed.

DOI: 10.1103/PhysRevB.82.144527 PACS number(s): 74.70.Xa, 76.75.+i, 74.25.Ha, 74.20.Mn

I. INTRODUCTION

The iron arsenide AFe_2As_2 systems (where A is an alkaline-earth element) crystallize with the tetragonal ThCr₂Si₂-type structure (space group *I4/mmm*). The interest for these compounds arises from the observation of superconductivity with transition temperatures T_c up to 38 K upon alkali-metal substitution for the A element²⁻⁴ or partial transition-metal substitution for iron.⁵ A huge number of studies were already devoted to unravel the properties of their superconducting ground state. However, some studies are hampered by the fact that to date no clear picture could be drawn about the bulk character of the superconductivity. For example, in superconducting systems obtained from the substitution of the A element (like K for Ba), muon-spin rotation/relaxation (µSR) measurements studies clearly indicate the occurrence of phase separation between magnetic and superconducting phases.⁶⁻⁸ On the other hand, substitution performed on the superconducting plane, as cobalt substitution for iron, does not reveal any phase separation as reported also by μSR .

The alkali-metal iron arsenide RbFe₂As₂ was discovered some years ago¹⁰ but was only recently found, by Bukowski et al., ¹¹ to exhibit type-II bulk superconductivity below $T_c \approx 2.6$ K. The reported studies were hindered by a limited temperature range of the equipment and the full development of the Meissner state could not be recorded. The estimated value of the upper critical field at zero temperature, $B_{c2} \approx 2.5$ T, was obtained from magnetization measurements performed at various field down to 1.5 K in the mixed state and by assuming a temperature dependence provided by the Werthamer-Helfand-Hohenberg theory. ¹¹

Compared to the better known compound BaFe₂As₂, RbFe₂As₂ possesses a lower Fermi level and is characterized by the absence of magnetic instability. Furthermore, the electron deficiency in RbFe₂As₂ leads also to a change (i.e., a decrease) in the number of bands contributing to the super-

conducting state, compared, for example, to $Ba_{1-x}K_xFe_2As_2$. Hence, one expects a strong decrease in the contribution of the electronlike bands at the M point of the Fermi surface. Such a decrease has been observed by angle-resolved photoemission spectroscopy¹² in the analog system KFe₂As₂, which also presents a case of naturally hole-(over)doped system when compared to the alkaline-earth "122" iron-based superconductors.

As exemplified by a number of recent studies, the μ SR technique is very well suited to investigate the superconducting properties of iron-based systems (see, for example, Ref. 13). In addition, due to its comparatively low upper critical field B_{c2} and its reduced T_c , the system RbFe₂As₂ opens a unique opportunity to fully study the B-T phase diagram of an iron-arsenide compound.

In this paper, we report on a detailed study of the temperature and field dependence of the magnetic penetration depth of RbFe₂As₂, which is closely related to the superconducting carrier concentration.

II. EXPERIMENT

Polycrystalline samples of RbFe₂As₂ were synthesized in two steps as reported recently. The μ SR measurements were performed at the π M3 beamline of the Paul Scherrer Institute (Villigen, Switzerland), using the general purpose spectrometer instrument (for temperatures down to 1.6 K and field up to 0.6 T) as well as the low temperature facility instrument (for temperatures down to 0.02 K and higher fields). Both zero-field (ZF) and transverse-field (TF) μ SR measurements were performed. Additional transport studies were performed on the very same sample at the ETH-Zürich using an ac transport option of a Quantum Design 14T-PPMS.

III. RESULTS AND DISCUSSION

To exclude the occurrence of any magnetic contributions of the Fe ions at low temperature, we performed first ZF

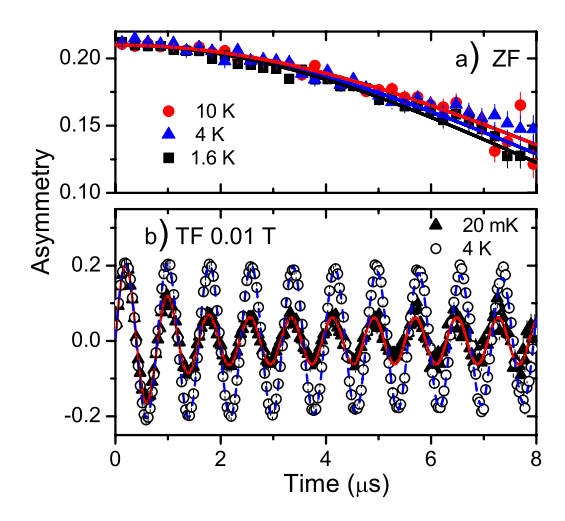


FIG. 1. (Color online) Typical μ SR spectra recorded above and below T_c , in: (a) zero field and (b) transverse field.

measurements above and below T_c . As exemplified by the data reported in Fig. 1(a), no sign of static magnetism could be detected on the ZF response RbFe₂As₂. The data are well described by a standard Kubo-Toyabe depolarization function, ¹⁴ reflecting the field distribution at the muon site created by the nuclear moments. The marginal increase in the depolarization rate, not related to the superconducting transition, possibly points to a slowing down of the magnetic fluctuations.

Figure 1(b) exhibits the TF μ SR time spectra measured in an applied field of 0.01 T, above (T=4 K) and below (T=0.02 K) the superconducting transition temperature. The strong muon-spin depolarization at low temperatures reflects the formation of the flux-line lattice (FLL) in the superconducting state. The long-lived component detectable at low temperatures is due to a background contribution from the sample holder. In a polycrystalline sample the magnetic penetration depth λ (and consequently the superconducting carrier concentration $n_s \propto 1/\lambda^2$) can be extracted from the Gaussian muon-spin depolarization rate $\sigma_s(T)$ [see also below Eq. (2)], which reflects the second moment (σ_s^2/γ_μ^2) of the magnetic field distribution due to the FLL in the mixed state. The TF data were analyzed using the polarization function

$$A_0 P(t) = A_s \exp\left[-\frac{(\sigma_s^2 + \sigma_n^2)t^2}{2}\right] \cos(\gamma_\mu B_{\text{int}}t + \varphi)$$
$$+ A_{\text{sh}} \exp\left(-\frac{\sigma_{\text{sh}}^2 t^2}{2}\right) \cos(\gamma_\mu B_{\text{sh}}t + \varphi). \tag{1}$$

The first term on the right-hand side of Eq. (1) represents the sample contribution, where A_s denotes the initial asymmetry connected to the sample signal; σ_s is the Gaussian relaxation rate due to the FLL; σ_n is the contribution to the field distribution arising from the nuclear moment and which is found to be temperature independent, in agreement with the ZF results; B_{int} is the internal magnetic field, sensed by the muons; and φ is the initial phase of the muon-spin ensemble. The second term reflects the muons stopping in the

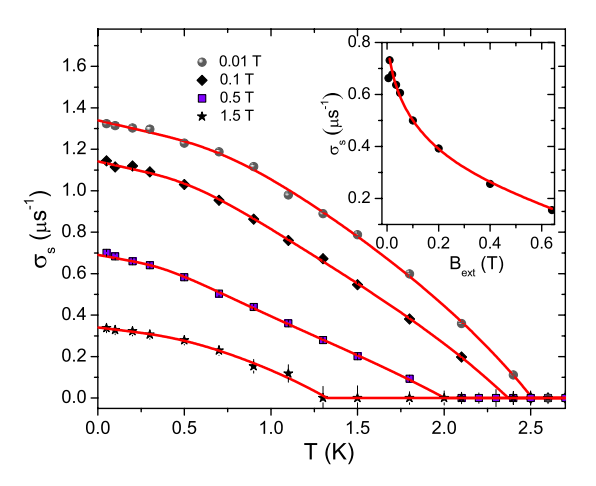


FIG. 2. (Color online) Temperature dependence of the depolarization rate due to the FLL in RbFe₂As₂ and obtained in fields of 1.5, 0.5, 0.1, and 0.01 T (lines are guides to the eyes). Inset: field dependence of σ_s obtained at 1.6 K and analyzed using the Eq. (2).

silver sample holder, where $A_{\rm sh}$ denotes the initial asymmetry connected to the holder signal; $\sigma_{\rm sh}$ is the relaxation rate due to the nuclear moments (which is very close to zero in this case); and $B_{\rm sh}$ is the magnetic field in the sample holder, which has essentially the value of the external field.

In Fig. 2, we report the temperature dependence of σ_s extracted from TF-µSR measurements in four different fields. We note first that the perfect fits obtained by assuming a Gaussian field distribution of the FLL point to a rather large anisotropy of the magnetic penetration depth in our system. This is confirmed by recent μ SR measurements performed on hole- and electron-doped 122 systems.^{8,9} As expected, σ_s is zero in the paramagnetic state and starts to increase below $T_c(B)$ when the FLL is formed. Upon lowering the temperature, σ_s increases gradually reflecting the decrease in the penetration depth or, alternatively, the increase in the superconducting density. The overall decrease in σ_s at very low temperatures observed upon increasing the applied field is a direct consequence of the decrease in the width of the internal field distribution when increasing the field toward B_{c2} . In order to quantify such an effect, one can make use of the numerical Ginzburg-Landau model, developed by Brandt. 15 This model allows one to calculate the superconducting carrier concentration with good approximation within the local (London) approximation ($\lambda \gg \xi$, ξ is the coherence length). This model predicts the magnetic field dependence of the second moment of the magnetic field distribution or, alternatively, of the µSR depolarization rate, which can be expressed as

$$\sigma_{\rm s} (\mu {\rm s}^{-1}) = 4.83 \times 10^4 (1 - B/B_{c2})$$

 $\times [1 + 1.21(1 - \sqrt{B/B_{c2}})^3] \lambda^{-2} ({\rm nm}).$ (2)

The field dependence of σ_s was measured down to 0.02 K and, as illustration, the inset of Fig. 2 exhibits the measurements at 1.6 K. For each data point, the sample was field cooled from above T_c and the recorded μ SR spectra were analyzed with Eq. (1). At each temperature, the field dependence of σ_s was analyzed with Eq. (2) by leaving the param-

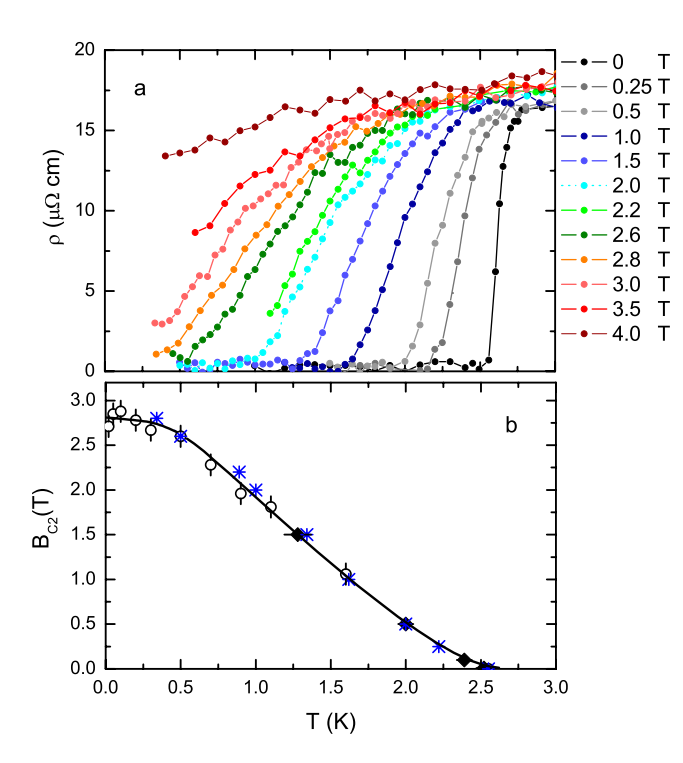


FIG. 3. (Color online) (a) Field dependence of the electrical resistivity. (b) Upper critical field for RbFe₂As₂. The open circles are obtained by analyzing the field dependence of σ_s using Eq. (2), as explained in the text. The diamonds are the value obtained by analyzing the temperature dependence of σ_s . The stars correspond to the complete disappearance of the resistivity in field. The line is a guide to the eyes.

eters λ and B_{c2} free. The corresponding fitted values of the penetration depth (related to the superconducting carrier concentration) and of the upper critical field are reported in Figs. 3(b) and 4. As demonstrated by Fig. 3(b), the values of B_{c2} obtained by fitting the field dependence of σ_s (assuming a field-independent penetration depth) agree very well with the values of B_{c2} obtained from the magnetoresistivity and the ones deduced directly from the temperature dependence of σ_s (see Fig. 2). This is a strong support that the assumption of a field-independent penetration depth is indeed valid. This rules out the possibility that RbFe₂As₂ is a nodal superconductor, since a field should have induced excitations at the gap nodes due to nonlocal and nonlinear effects, thus reducing the superconducting carrier concentration n_s and therefore affecting λ (see, for example, Ref. 16).

By looking at the temperature dependence of λ^{-2} obtained using Eq. (2) with the values of the parameter $B_{c2}(T)$ presented in Fig. 3(b), the zero-temperature value of the penetration depth $\lambda(0)=267(5)$ nm can be deduced. The obtained temperature dependence of λ^{-2} was analyzed, in a first step, within the framework of a BCS single s-wave symmetry superconducting gap Δ (see Fig. 4), using the form¹⁷

$$\frac{\lambda^{-2}(T)}{\lambda^{-2}(0)} = 1 - \frac{2}{k_{\rm B}T} \int_{\Lambda}^{\infty} f(\epsilon, T) [1 - f(\epsilon, T)] d\epsilon, \tag{3}$$

where $f(\epsilon, T) = (1 + \exp[\sqrt{\epsilon^2 + \Delta(T)^2}/k_BT])^{-1}$ and with a standard BCS temperature dependence for the gap function. As

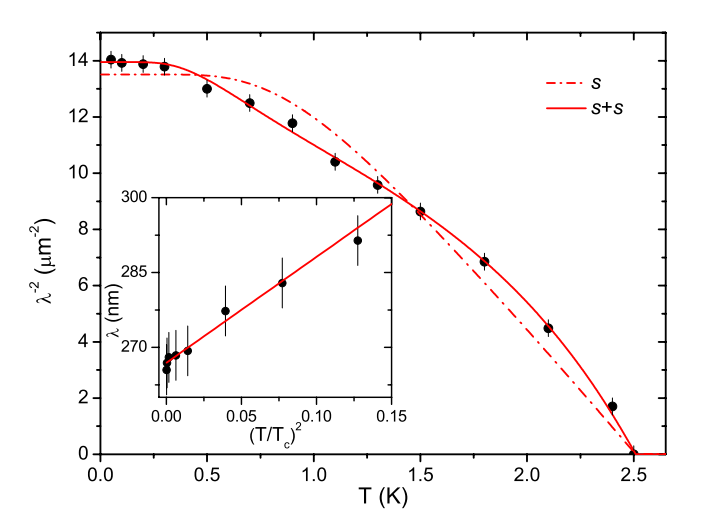


FIG. 4. (Color online) Magnetic penetration depth as a function of temperature. Above 0.5 K, the values obtained with Eq. (2) coincides with the values measured in a field of 0.01 T, and only these latter are plotted for this temperature range. The red dashed line corresponds to a BCS s-wave gap symmetry whereas the solid one to represents a fit using a two-gap s+s model. The inset exhibits the penetration depth as a function of $(T/T_c)^2$.

evidenced in Fig. 4, this analysis is not satisfactory. We note also that a d-wave symmetry model does not fit the data, confirming at *posteriori* the discussion of a field-independent penetration depth. These results are actually not unexpected, as there are growing evidences that several disconnected Fermi-surface sheets contribute to the superconductivity, as revealed by angle-resolved photoemission spectroscopy, ¹² resulting into two distinct values of superconducting gaps. Hence, in a second step, the experimental $\lambda^{-2}(T)$ data were analyzed by assuming two independent contributions with different values Δ_i of s-wave gaps. 8,18,19 In Fig. 4 the solid line shows a s+s multigap function which fits to the experimental data rather well. The parameters extracted from the fit are $\Delta_1(0)=0.15(2)$ meV for the small gap value (contributing $\omega = 36\%$ to the total amount of n_s) and Δ_2 =0.49(4) meV for the larger one. However, note that according to Eq. (3), λ^{-2} is insensitive to the phase of the superconducting gap(s). By considering the intrinsic hole doping in RbFe₂As₂ compared to the optimally doped 122 iron-based system, it is natural to consider that the gaps values are connected, respectively, to the outer (β) and inner (α) holelike bands at the Γ point of the Fermi surface. In this frame, RbFe₂As₂ can be considered as hole overdoped with electronlike γ and δ bands at the M point, which shift to the unoccupied side. Note that in optimally doped 122 systems, one observes the occurrence of ϵ hole bands (so-called "blades") around the M point, which also slightly contribute to the superconducting carrier concentration.

An additional support for a two-gap superconducting state could be provided by the observed positive curvature of the $B_{c2}(T)$ near T_c , in sharp contrast to the usual B_{c2} BCS temperature dependence [see Fig. 3(b)]. Note first that the values of B_{c2} extracted from the fit with Eq. (2) are in perfect agreement with: (i) the values corresponding to the complete suppression of the electrical resistivity in field and (ii) to the

values obtained by analyzing the temperature dependence of σ_s in different magnetic fields (see Fig. 2). An additional indication that bulk superconductivity occurs when the electrical resistivity completely vanishes is provided by specificheat measurements²⁰ performed in zero-applied field for which the observed T_c corresponds to 2.52(1) K.

Similar positive curvature of the $B_{c2}(T)$ near T_c were observed in MgB₂ (Refs. 21 and 22) and in the borocarbides,²³ where it was explained within a two-gap model. However, one should keep in mind that alternative explanations for the observed positive curvature in $B_{c2}(T)$ are possible and that complementary measurements, as here our $\lambda^{-2}(T)$ data, are necessary to draw conclusions.

If on one hand, the two-gap model scenario appears to best fit the temperature dependence of the penetration depth, on the other hand one could argue that it does not appear fully consistent with the observation that the field evolution of the field distribution follows Eq. (2). Hence for a two-gap model, one expects a deviation from the simple field dependence reflecting the occurrence of distinct lengths scales ξ_i for both gaps (associated to the coherence length, for a clean single gap system). Such behavior is, for example, clearly observed on the archetypical two-gap superconductor MgB₂.²⁴ The experimental observation that Eq. (2) reproduces our data indicates a small difference between the ξ_i parameters for both bands. This is also inline with the very good agreement between the extracted values of B_{c2} with Eq. (2) and the observed values by resistivity. In this frame, we also mention that ARPES measurements²⁵ on members of the 122 family indicate that the Fermi velocity of the inner Γ -barrel band (α band) is substantially higher that the one for the outer Γ -barrel band (β band), which therefore weakens the difference of the gap values on the ξ_i parameters (as ξ $\propto \langle v_{\rm F} \rangle / \Delta$). Finally, we note that the observed depolarization rate in RbFe₂As₂ is about 40 times weaker than the one reported for MgB₂, hampering therefore the determination of possible distinct ξ_i length scales.

For completeness, we discuss now the slight deviation observed at very low temperatures from the s+s fit and the $\lambda^{-2}(T)$ data. Recently, it was shown that the observation of universal scalings in the whole iron-pnictides superconductors, for the specific-heat jump $(\Delta C \propto T_c^3)$ and the slope of upper critical field at $T_c(dB_{c2}/dT \propto T_c)$ could be interpreted as signatures for strong pair-breaking effects, ²⁶ as, for example, magnetic scattering. In the same frame it was deduced that such an effect should lead to a very low-temperature dependence of the penetration depth deviating from an usual exponential behavior and transforming into a

quadratic one, i.e., $\lambda \propto T^2$, which is indeed reported in a number of studies (see, for example, Refs. 28 and 29). In the inset of Fig. 4 we report the extracted penetration depth as a function of $(T/T_c)^2$. The good scaling is inline with the presence of magnetic scattering in RbFe₂As₂, as previously reported for hole- or electron-doped 122 systems.²⁷

IV. CONCLUSION

To conclude, µSR measurements were performed on a RbFe₂As₂ polycrystalline sample. From the temperature and field dependence of the superconducting response of the μ SR signal, the values of the upper critical field and of the magnetic penetration depth could be extracted. The zerotemperature values of $B_{c2}(0)$ and $\lambda(0)$ were estimated to be 2.6(2) T and 267(5) nm, respectively. The temperature dependence of the penetration depth and similarly of the superconducting carrier concentration are reproduced assuming a multigap model with possibly pair-breaking effects at low temperatures. The multigap scenario is supported by the observation of a clear positive curvature on the temperature dependence of the upper critical field. We attribute these gaps to the holelike bands around the Γ point of the Fermi surface and possibly also to the hole-bands blades around the M point. Assuming that the γ and δ electronlike bands around the M point are in the unoccupied side, one would expect an absence of nesting conditions in RbFe₂As₂. The consequence would be an absence of magnetic order, as confirmed by our ZF data, and a strong decrease in the interband processes between the α and $\gamma(\delta)$ bands. In this frame, it is remarkable to see that the ratio between the gaps values is decreased by a factor more than 2 compared to optimally doped 122 systems. Similarly, we note that the BCS ratio $2\Delta/k_{\rm B}T_{\rm c}$ for the small gap that we assign to the β band is almost identical to the values observed for optimally doped $Ba_{1-x}K_xFe_2As_2$, i.e., $2\Delta_1/k_BT_c \approx 1.4$. On the other side, for the large gap of the α band, this ratio is strongly reduced, 8,25 confirming therefore the possible role played by interband processes in optimally hole-doped iron-based 122 superconductors.

ACKNOWLEDGMENTS

Part of this work was performed at the Swiss Muon Source ($S\mu S$), Paul Scherrer Institute (PSI, Switzerland). The work of M.B. was supported by the Swiss National Science Foundation. The work at the IFW Dresden has been supported by the DFG through FOR 538.

¹M. Pfisterer and G. Nagorsen, Z. Naturforsch. B 35, 703 (1980).

²M. Rotter, M. Tegel, and D. Johrendt, Phys. Rev. Lett. **101**, 107006 (2008).

³K. Sasmal, B. Lv, B. Lorenz, A. M. Guloy, F. Chen, Y.-Y. Xue, and C.-W. Chu, Phys. Rev. Lett. **101**, 107007 (2008).

⁴Z. Bukowski, S. Weyeneth, R. Puzniak, P. Moll, S. Katrych,

N. D. Zhigadlo, J. Karpinski, H. Keller, and B. Batlogg, Phys. Rev. B **79**, 104521 (2009).

⁵A. S. Sefat, R. Jin, M. A. McGuire, B. C. Sales, D. J. Singh, and D. Mandrus, Phys. Rev. Lett. **101**, 117004 (2008).

⁶ A. A. Aczel, E. Baggio-Saitovitch, S. L. Budko, P. C. Canfield, J. P. Carlo, G. F. Chen, P. Dai, T. Goko, W. Z. Hu, G. M. Luke,

- J. L. Luo, N. Ni, D. R. Sanchez-Candela, F. F. Tafti, N. L. Wang, T. J. Williams, W. Yu, and Y. J. Uemura, Phys. Rev. B 78, 214503 (2008).
- ⁷J. T. Park, D. S. Inosov, Ch. Niedermayer, G. L. Sun, D. Haug, N. B. Christensen, R. Dinnebier, A. V. Boris, A. J. Drew, L. Schulz, T. Shapoval, U. Wolff, V. Neu, X. Yang, C. T. Lin, B. Keimer, and V. Hinkov, Phys. Rev. Lett. 102, 117006 (2009).
- ⁸R. Khasanov, D. V. Evtushinsky, A. Amato, H.-H. Klauss, H. Luetkens, Ch. Niedermayer, B. Büchner, G. L. Sun, C. T. Lin, J. T. Park, D. S. Inosov, and V. Hinkov, Phys. Rev. Lett. 102, 187005 (2009).
- ⁹R. Khasanov, A. Maisuradze, H. Maeter, A. Kwadrin, H. Luetkens, A. Amato, W. Schnelle, H. Rosner, A. Leithe-Jasper, and H.-H. Klauss, Phys. Rev. Lett. 103, 067010 (2009).
- ¹⁰A. Czybulka, M. Noack, and H.-U. Schuster, Z. Anorg. Allg. Chem. **609**, 122 (1992).
- ¹¹Z. Bukowski, S. Weyeneth, R. Puzniak, J. Karpinskia, and B. Batlogg, Physica C (to be published).
- ¹²T. Sato, K. Nakayama, Y. Sekiba, P. Richard, Y.-M. Xu, S. Souma, T. Takahashi, G. F. Chen, J. L. Luo, N. L. Wang, and H. Ding, Phys. Rev. Lett. **103**, 047002 (2009).
- ¹³ A. Amato, R. Khasanov, H. Luetkens, and H.-H. Klauss, Physica C 469, 606 (2009).
- ¹⁴R. Kubo and T. Toyabe, *Magnetic Resonance and Relaxation* (North-Holland, Amsterdam, 1967).
- ¹⁵E. H. Brandt, Phys. Rev. B **68**, 054506 (2003).
- ¹⁶M. H. S. Amin, M. Franz, and I. Affleck, Phys. Rev. Lett. **84**, 5864 (2000).
- ¹⁷M. Tinkham, *Introduction to Superconductivity* (McGraw-Hill., New York, 1996).

- ¹⁸C. Niedermayer, C. Bernhard, T. Holden, R. K. Kremer, and K. Ahn, Phys. Rev. B **65**, 094512 (2002).
- ¹⁹ A. Carrington and F. Manzano, Physica C **385**, 205 (2003).
- ²⁰J. Kanter (private communication).
- ²¹O. F. de Lima, R. A. Ribeiro, M. A. Avila, C. A. Cardoso, and A. A. Coelho, Phys. Rev. Lett. **86**, 5974 (2001).
- ²²A. V. Sologubenko, J. Jun, S. M. Kazakov, J. Karpinski, and H. R. Ott, Phys. Rev. B 65, 180505 (2002).
- ²³ S. V. Shulga, S.-L. Drechsler, G. Fuchs, K.-H. Müller, K. Winzer, M. Heinecke, and K. Krug, Phys. Rev. Lett. **80**, 1730 (1998).
- ²⁴S. Serventi, G. Allodi, R. De Renzi, G. Guidi, L. Romanò, P. Manfrinetti, A. Palenzona, Ch. Niedermayer, A. Amato, and Ch. Baines, Phys. Rev. Lett. **93**, 217003 (2004).
- ²⁵D. V. Evtushinsky, D. S. Inosov, V. B. Zabolotnyy, M. S. Viazovska, R. Khasanov, A. Amato, H.-H. Klauss, H. Luetkens, Ch. Niedermayer, G. L. Sun, V. Hinkov, C. T. Lin, A. Varykhalov, A. Koitzsch, M. Knupfer, B. Büchner, A. A. Kordyuk, and S. V. Borisenko, New J. Phys. 11, 055069 (2009).
- ²⁶V. G. Kogan, Phys. Rev. B **80**, 214532 (2009).
- ²⁷R. T. Gordon, H. Kim, M. A. Tanatar, R. Prozorov, and V. G. Kogan, Phys. Rev. B **81**, 180501(R) (2010).
- ²⁸C. Martin, M. E. Tillman, H. Kim, M. A. Tanatar, S. K. Kim, A. Kreyssig, R. T. Gordon, M. D. Vannette, S. Nandi, V. G. Kogan, S. L. Bud'ko, P. C. Canfield, A. I. Goldman, and R. Prozorov, Phys. Rev. Lett. 102, 247002 (2009).
- ²⁹ H. Kim, C. Martin, R. T. Gordon, M. A. Tanatar, J. Hu, B. Qian, Z. Q. Mao, R. Hu, C. Petrovic, N. Salovich, R. Giannetta, and R. Prozorov, Phys. Rev. B 81, 180503(R) (2010).